

A study of the interstellar medium in line to NGC 5128 from high resolution observations of the supernova 1986G^{*}

S. D'Odorico¹, S. di Serego Alighieri^{2, **}, M. Pettini³, P. Magain¹, P. E. Nissen⁴, and N. Panagia^{5, **}

¹ European Southern Observatory, Karl-Schwarzschild-Strasse 2, D-8046 Garching, Federal Republic of Germany

² Space Telescope European Coordinating Facility, Karl-Schwarzschild-Strasse 2, D-8046 Garching, Federal Republic of Germany

³ Anglo-Australian Observatory, Epping Laboratory, P.O. Box 296, Epping, NSW 2121, Australia

⁴ Institute of Astronomy, University of Aarhus, DK-8000 Aarhus C, Denmark

⁵ Space Telescope Science Institute, 3700 San Martin Drive, Baltimore, MD 21218, USA

Received August 5, accepted November 17, 1988

Summary. We present new high resolution, high S/N ratio spectra of supernova 1986G in NGC 5128 (Cen A). These data allow a detailed study of the rich interstellar absorption spectrum originating in the line of sight to the SN. At least 12 distinct Ca II and Na I absorbing clouds are identified. The gas associated with NGC 5128 is spread over a velocity range of 178 km s^{-1} and it is split in at least 7 components. A new result unique to NGC 5128 is the presence of 3 components with Ca^+/Na^0 column densities ratios smaller than 1, that is typical of cool disc gas. This is interpreted as a further indication of the existence of an extended warped disc or a ring of cool gas.

From the discussion of the velocities of the absorption components seen in its spectrum it is inferred that the SN was at least half way within the dust and gaseous disc of the galaxy.

An intriguing result of this work is the discovery of two absorption components at $v_H = 236$ and 257 km s^{-1} , which cannot be easily explained within the velocity field of either the Galaxy or NGC 5128, and may be related to high velocity clouds of neutral hydrogen observed at nearby lines of sight.

We detected and measured several diffuse interstellar bands at galactic and NGC 5128 velocities. This is the first time that such a detailed study has been done in a galaxy beyond the Magellanic Clouds. At NGC 5128 velocities, we also detected, for the first time beyond the Local Group, molecular absorption lines of CH and CH^+ at optical wavelengths.

Key words: interstellar medium – galaxies: NGC 5128 – supernovae

1. Introduction

The last few years have seen a growing interest in using extragalactic supernovae (SN) as background probes of the intervening interstellar medium. This is due in large part to the availability of modern, high-throughput spectrographs and detectors and to the increasing success rate in discovering supernovae near maximum light. As a recent example, Jenkins et al. (1984) and D'Odorico, Pettini and Ponz (1985; hereafter referred to as DPP) were able to capitalize on the discovery of the bright ($V_{\text{max}} \approx 11.6$) SN 1983N in M83 by Evans (1983) to record, at high signal-to-noise and at a spectral resolution of $10\text{--}15 \text{ km s}^{-1}$ FWHM, the interstellar doublet lines of Ca II and Na I formed over the extended sight-line to this galaxy. Absorbing components due to interstellar gas in the disk and halo of both the Milky Way and M83 were revealed as well as absorption at intermediate velocities which may be plausibly attributed to intergalactic gas.

The subsequent discovery, also by Evans (1986), of the bright ($V \approx 12$ at the time of discovery) supernova 1986G in Centaurus A (NGC 5128) on 1986 May 3.5 UT, was thus particularly exciting as it provided a valuable opportunity to continue and extend this work to a nearby direction. At galactic coordinates $l = 309.54$, $b = +19.40$ (Cragg, 1986) the sight-line to SN 1986G in NGC 5128 is separated by only 13.3 degrees from the direction of SN 1983N in M83. NGC 5128 is the dominant member of the Centaurus group, a loose association of galaxies which includes M83; de Vaucouleurs (1979) estimates a distance $d = 3.3 \text{ Mpc}$ to both galaxies, while Sandage and Tammann (1975) give $d = 8.5 \text{ Mpc}$.

Figure 1 is a reproduction from a photographic plate of NGC 5128 obtained shortly after the supernova event. SN 1986G, later identified as type Ia (Phillips et al., 1987), can be seen to be located in the middle of the dust lane which is a characteristic feature of this galaxy. Cen A is the nearest giant double radio source and, without doubt, one of the most extensively studied objects in the sky, from radio wavelengths to gamma rays over 16 decades of the electromagnetic spectrum. Jet-like structures have been found to extend from the nucleus out to distances of

Send offprint requests to: S. D'Odorico

^{*} Based on observations made at the European Southern Observatory

^{**} Affiliated to the Astrophysics Division, Space Science Department of the European Space Agency

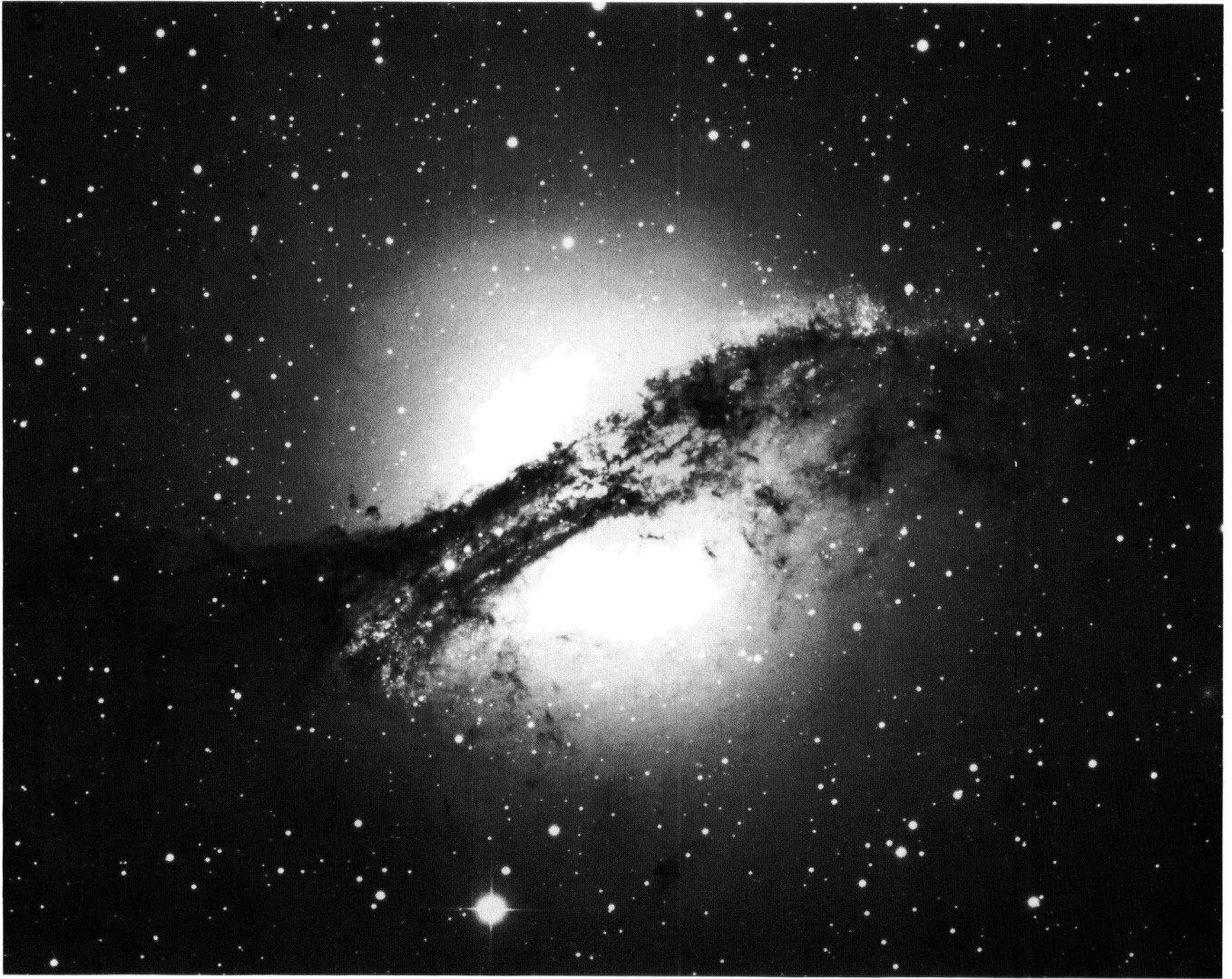


Fig. 1. Reproduction of a photographic plate obtained by D. Malin on 1986 May 31st at the prime focus of the AAT showing Cen A. North is at the top, east to the left. 85 min exposure on Kodak IIIaJ with a filter which gives true *B* band on J plates. Supernova 1986G is the brightest star in the middle of the south-east section of the dust lane

~ 40 kpc. Apart from its nuclear activity and central dust lane, the galaxy NGC 5128 is peculiar in that it consists of a young disk system, seen at an inclination of 73° , which includes stars, gas and dust and rotates rapidly about the major axis of an otherwise apparently normal elliptical galaxy. A comprehensive review of observations and models proposed for Cen A has been given by Ebner and Balick (1983). More recently, detailed studies of the stellar and gas dynamics have been carried out by Bertola et al. (1985), Wilkinson et al. (1986) and Bland et al. (1987). Thus, apart from providing an interesting comparison with the M83 sight-line, SN 1986G offered the ephemeral opportunity to obtain a unique view of the low-ionization component of the interstellar medium in the energetic environment of Cen A.

For these reasons, the news of the discovery of the supernova was promptly relayed to La Silla where two of us (P.N. and P.M.) were able to carry out high resolution spectroscopic observations on each night from May 7 to May 11 using CASPEC, the echelle spectrograph at the Cassegrain focus of the 3.6 m telescope. The resulting spectra are of excellent signal to noise (S/N) ratio and show strong interstellar absorption lines of Na I and Ca II at

velocities appropriate to NGC 5128, thus confirming that the supernova is located well within, if not behind, the gaseous disc of the galaxy. The analysis of these interstellar features is the subject of this paper.

The observations and data reduction procedure are described in Sect. 2 below. In Sect. 3 we analyze the profiles of the interstellar lines and derive physical parameters for the different gas clouds in line of sight. We also identify a number of diffuse interstellar bands (DIBs) and molecular lines at galactic and NGC 5128 velocities. In Sect. 4 we discuss these results and consider their implications; finally, in Sect. 5 we summarize the major conclusions and outline the prospects for future work.

2. Observations and data reduction

The observations were carried out with the European Southern Observatory (ESO) echelle spectrograph, CASPEC, at the $f/8$ Cassegrain focus of the 3.6 m telescope at La Silla, Chile. The journal of observations and details of the instrumental set up are

Table 1. CASPEC observations of SN1986G

| Observer | Date, average U.T. | Central wavelength (Å) | Exp. (min) | Slit (arcsec) |
|--------------|--|------------------------------|---------------|------------------|
| <i>Na I</i> | | | | |
| P. E. Nissen | 7 May, 4 ^h 50 ^m | 5800 | 60 | 2 |
| P. E. Nissen | 8 May, 2 ^h 00 ^m | 5800 | 60 | 1.5 |
| P. Magain | 11 May, 2 ^h 03 ^m | 6000 | 60 | 1.6 |
| P. Magain | 11 May, 3 ^h 12 ^m | 6000 | 60 | 1.6 |
| <i>Ca II</i> | | | | |
| P. E. Nissen | 9 May, 2 ^h 45 ^m | 4200 | 60 | 1.7 |
| P. E. Nissen | 9 May, 3 ^h 55 ^m | 4200 | 60 | 1.7 |
| P. Magain | 10 May, 2 ^h 55 ^m | 4300 | 90 | 1.6 |
| P. Magain | 10 May, 4 ^h 31 ^m | 4300 | 90 | 1.6 |
| P. Magain | 10 May, 5 ^h 45 ^m | 4300 | 45 | 1.6 |
| P. E. Nissen | 8 May, 3 ^h 20 ^m | 8500 | 60 | 1.5 |

given in Table 1. The instrument has been described by D'Odorico and Tanné (1984). For the observations presented here both a 31.6 lines mm⁻¹ and a 52 lines mm⁻¹ echelle grating were used in combination with a 300 lines mm⁻¹ grating cross disperser. A short-focal-length camera ($f/1.46$) focuses the beam onto a thinned, back-illuminated RCA CCD with 320 × 512 30 μm² pixels. One pixel on the detector corresponds to an entrance aperture of 1'2 × 0'7 on the sky, the first dimension being in the direction of the dispersion. ESO CCD chip number 3 was used in May 1986; its quantum efficiency is 50% and 80% at 3950 and 5900 Å respectively.

One CCD frame covers a spectral region approximately 900 Å wide, distributed over a few spectral orders; different spectral regions are brought into the CCD by remotely controlled motion of the cross-disperser. The observations of SN1986G were primarily aimed at securing high signal-to-noise, high resolution spectra in the regions of the interstellar lines of Ca II $\lambda\lambda$ 3933.663, 3968.468 (K and H) and Na I $\lambda\lambda$ 5889.950, 5895.924 (D₂ and D₁). Two separate exposures were necessary to record the two doublets. The 52 lines/mm echelle grating was used for the observations on May 10. With this grating the interorder spacing is a factor of two larger than with the 31.6 lines mm⁻¹ grating, and the intensity of interorder scattered light is substantially reduced, making the determination of the background more straightforward.

At the time of the CASPEC observations the brightness of the supernova in the *V* and *B* bands was still increasing slightly, in ranges 11.7–11.5 (*V*) and 12.7–12.5 (*B*), according to the measurements reported by Feast and Phillips (1986), Bues et al. (1986) and Blanco (1986). The corresponding mean count rates in our spectra were 20 and 2.1 electrons per second per wavelength bin (corresponding to 1 pixel in the direction of the dispersion) is 0.18 Å and 0.12 Å respectively. For each observation in Table 1, a flat field image produced by a quartz lamp and the comparison spectrum of a thorium-argon hollow cathode lamp were also recorded.

The spectra were flat fielded, extracted and wavelength calibrated with the echelle data reduction package implemented within MIDAS, the image processing system running at ESO on the VAX 8600 computer, in the manner described by Ponz et al.

(1986). The error in the wavelength calibration was inferred from the standard deviation of the third order polynomial fitting the comparison lines to be better than ± 2 km s⁻¹. The error in the absolute velocity determinations from CASPEC spectra is also generally of the order of 2 km s⁻¹ (D'Odorico and Ponz, 1984). The final spectral resolution of the data was measured from the FWHM of emission lines from the comparison lamp and from the λ 5577 [O I] sky line. For the Na I and Ca II spectral regions the FWHM are 15 and 17 km s⁻¹, respectively.

The different spectra matched very well in wavelength and intensity. A straight average was made of the spectra with the same resolution and comparable S/N ratios. For the red spectral region the observations of May 11 and 8 were used, for the blue those of May 9 and the first two of May 10.

Finally, portions of the SN spectrum in the proximity of the interstellar lines were fitted with a number of splines (between 4 and 6) so as to define the underlying continuum level; division of the data by this then produced the normalized profiles shown in Fig. 2. The measured rms deviation of the data points from the fitted continuum is used to estimate the signal-to-noise ratio attained, which for the data of Fig. 2 is 110, 80, and 250 for the Ca II K, Ca II H, and Na I D lines, respectively.

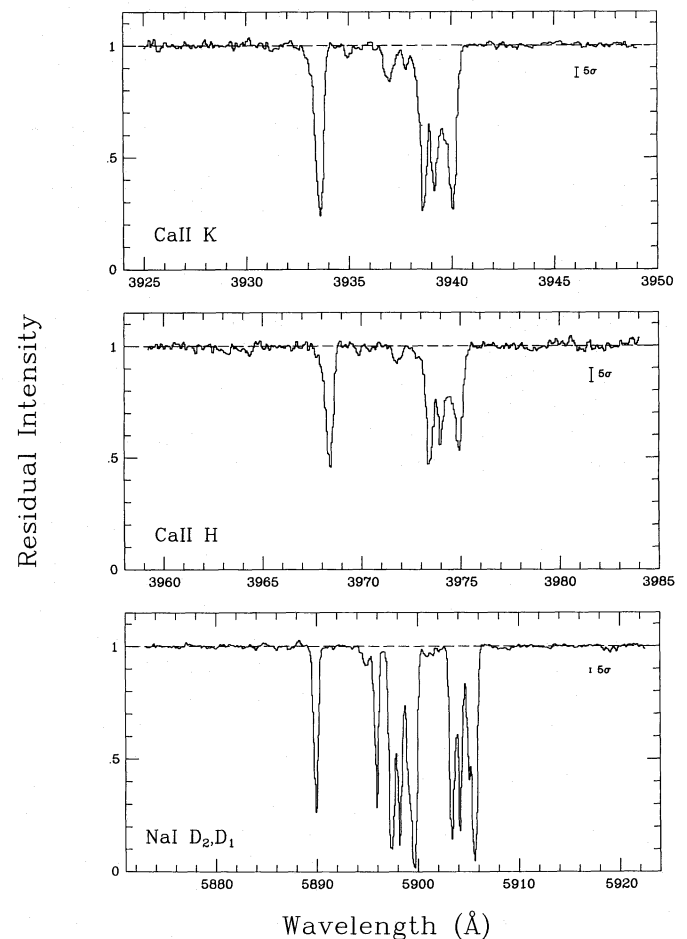


Fig. 2. Normalized portions of the spectrum of SN1986G encompassing the interstellar Ca II and Na I lines. The vertical bar shown in each panel corresponds to five times the measured rms deviation of the data from the continuum level. The corresponding signal-to-noise ratios are between ~ 80 and ~ 250 ; the spectral resolution is ~ 16 km s⁻¹ FWHM. Many weak absorption features due to atmospheric water vapour are present in the region of the Na I D doublet lines

3. The interstellar spectrum of SN 1986G

3.1. Ca II and Na I absorbing clouds

As can be seen from Fig. 2, the interstellar lines formed along the extended path length to the supernova show a complex structure with several absorption components spanning a velocity interval of over 500 km s^{-1} .

The high resolution and signal-to-noise ratio of our data allow a detailed analysis of the profiles of the interstellar lines from which the physical parameters of the absorbing clouds can be deduced. The analysis uses the same absorption-line analysis software package (ALAS) employed by DPP in their study of the interstellar spectrum of SN 1983N. Briefly, the distribution of the velocities of the absorbing matter in the line of sight is assumed to be the sum of individual gaussian components, each defined by a central velocity v_i , a velocity dispersion b_i and a column density N_i of absorbing ions. A theoretical absorption profile is computed for an initial set of values of v_i , b_i , and N_i and compared with the observed line profile after convolution with the instrumental broadening function, which in our case is assumed to be also a gaussian with FWHM as measured from emission lines in the comparison spectrum. Through an iterative process, the parameters of the cloud model are subsequently adjusted until an optimum fit to the observations is obtained by minimizing the sum of the squares of the residuals between observed and computed profiles. The degrees of freedom in the profile fitting method are limited by two constraints. First, the two members of each doublet were fitted together so as to derive self-consistent results for Ca II and Na I. Secondly, in the iterative search for the best fitting model, the number of clouds was kept to a minimum, so that only components which are at least partially resolved were included in the fit.

The final model fits are shown as continuous lines in Fig. 3 superposed on the observed data points (dots). The parameters of the model fits are collected in Table 2, where for each component we give the heliocentric velocity v_H , the velocity dispersion b , the column density N and the values of equivalent width W_λ computed with these parameters. For comparison we also give in the last two columns of Table 2 the *measured* equivalent widths for each component, or group of components, which is fully resolved in our spectra.

From Fig. 3 and Table 2 it can be seen that we identify 12 absorption components in Ca II, 9 of which are also seen in Na I. As discussed in detail in Sect. 4 below, the velocities of components 1, 2, and 3 are consistent with an origin in gas in our Galaxy, while components 8, 9, 10, 11, and 12 (and possibly also 6 and 7) occur at velocities appropriate to interstellar clouds in Cen A. Interestingly, we also find absorption at velocities intermediate between those of the two galaxies (components 4 and 5).

In general, the correspondence between the parameters of the Ca II and Na I cloud models is good, with only components 2 and 12 differing in velocity by as much as $5\text{--}6 \text{ km s}^{-1}$ between the two species. Nevertheless, the strongest absorption features (numbers 2, 8, 9, and 12) are probably blends of yet more unresolved components, as suggested by the fact that the b -values required to fit the Na I D lines are consistently lower than those deduced for Ca II H and K. These components are remarkably strong, with observed residual intensities lower than $\sim 20\%$ in Na I, indicative of an origin in moderately dense interstellar clouds in the disk of the Milky Way and NGC 5128. Because of this, the column densities deduced for components 2, 8, 9, and 12 are strictly lower limits, since additional absorption by gas with very low velocity

dispersions ($b \leq 1 \text{ km s}^{-1}$) could easily be masked by the broader components we resolve (Nachman and Hobbs, 1973). For the other, weaker components of the Ca II and Na I lines, extensive trials with the parameters of the profile fits indicated that the values of column density given in Table 2 are unlikely to be in error by more than 30% (depending on the strength of the absorption and the degree of blending). Components 1, 3, and 7 are below our detection limit in Na I; the corresponding upper limits to $N(\text{Na}^0)$ were deduced adopting the b -values derived from the Ca II lines and from consideration of the strength of nearby noise features, of possible contamination by telluric water-vapour absorption, and of blending with other interstellar components. Table 3 lists the column density ratios $N(\text{Ca}^+)/N(\text{Na}^0)$ (or lower limits) for the 12 components.

Rich (1987) had also obtained spectra of the SN at comparable resolution in the region of the Na I interstellar lines, using the echelle spectrograph at the CTIO 4 m-telescope. His observations were taken approximately 45 days after maximum light, when the visual magnitude of the supernova was about 14.1. The decrease by a factor of 10 in apparent brightness explains the lower signal-to-noise ratio of his observation with respect to ours. He detects the four strongest absorption components in NGC 5128 only; the velocities are in excellent agreement with our measurements but for a shift of $+3 \text{ km s}^{-1}$ in the velocity scale.

3.2. The interstellar bands

While the present observations of SN 1986G were aimed primarily at obtaining the Na I and Ca II absorption line regions, they also led to the discovery of a number of diffuse interstellar bands (DIBs) both at galactic and extragalactic velocities.

The nature of the carrier or carriers of the DIBs represents one of the longest standing unsolved problems in astronomy, even though these features were first recognized over fifty years ago (Merrill, 1934). Both a solid state interpretation, that is based on interstellar grain as the $\lambda 2175$ feature, and a molecular origin have been proposed. For a taste of the extensive and often controversial literature on this subject and for references to earlier work on the subject, we refer to the discussion by Pettini and D'Odorico (1986).

Detections of DIBs outside the Galaxy have been few and confined to the Magellanic Cloud. In particular, the recent observations of the bright supernova in the LMC, 1987A, have provided a new set of accurate measurements toward the 30 Dor region (Vladilo et al., 1987). Bright supernovae in early stages of evolution are ideal background sources for this type of investigation as their spectra are free from the narrow features which can hinder the measurement of DIBs in stellar spectra.

The detection of DIBs in the dust-rich system NGC 5128 is promising since a comparative study of these features in galaxies of different gas and dust content such as the Galaxy, the LMC and Cen A may provide new clues as to the nature of the carriers.

For a systematic search of diffuse bands in the spectra of SN 1986G we used the list given in Table 1 of Herbig (1975). The spectral ranges covered by our spectra ($3800\text{--}4800 \text{ \AA}$ and $5300\text{--}6500 \text{ \AA}$) overlap well with a large fraction of Herbig's survey, and the data are of comparable resolution and signal-to-noise ratio. However, in the case of our spectra, two additional difficulties are encountered. First, since one echelle order encompasses only $80\text{--}100 \text{ \AA}$, the continuum level cannot be determined accurately in the presence of broad, shallow features with $\text{FWHM} \geq 10 \text{ \AA}$. This makes the identification and measurement of the broader diffuse bands difficult. Second, no observations of a smooth-spectrum

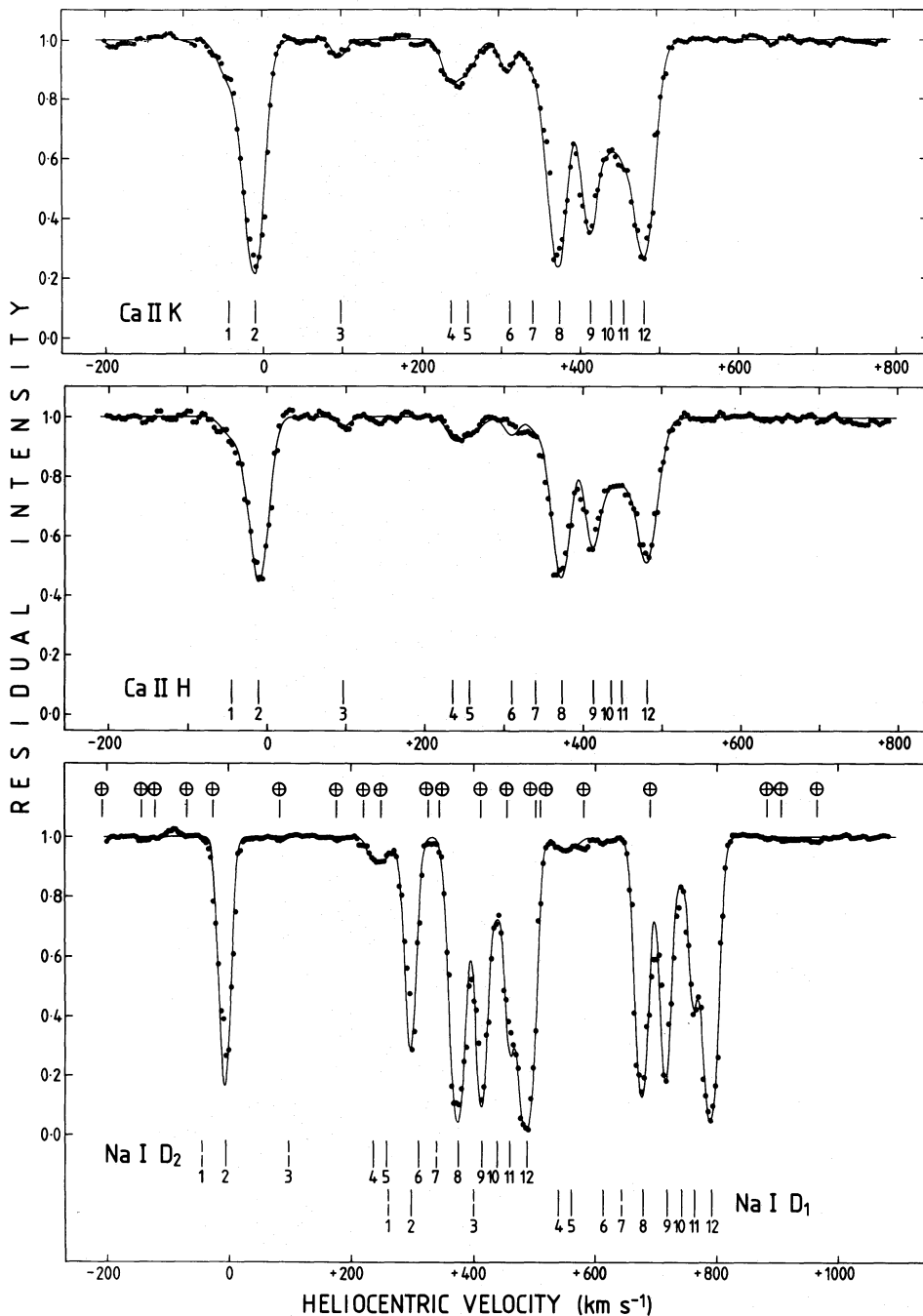


Fig. 3. Comparison between observed (dots) and computed (thin continuous line) profiles of interstellar lines towards SN 1986G. The numbered tick marks identify the individual components contributing to the complex absorption profiles, as detailed in Table 2. (Broken ticks in the bottom panel indicate the locations of components identified in Ca II, but below the detection limit in Na I). The velocity scale of the bottom panel refers to the D₂ line. The symbols ⊕ above the Na I spectrum mark the positions of telluric water vapour lines contaminating this region; however, the equivalent widths of these weak absorption features are typically only a few mÅ

star were obtained which could provide a template for correcting for atmospheric absorption by H₂O and O₂. Telluric lines do seriously affect regions in the red spectrum where some of the DIBs are located.

The search for the diffuse bands was carried out by overlapping the expected positions of the components detected in Na I to the normalized spectra of SN 1986G at the wavelength of each band of Class A in the list by Herbig (1975). For galactic gas, DIBs may be expected to be centered near $v_H = -6.5 \text{ km s}^{-1}$, the velocity of the strongest Na I absorption (component 2 in Table 2 and Fig. 3); similarly, the strongest components in NGC 5128 (8, 9, and 12, at $v_H = 375, 414,$ and 488 km s^{-1}) may plausibly show associated DIB features.

Table 4 lists the bands which have been positively identified at galactic and/or Cen A velocities, together with their measured equivalent widths. The errors are dominated by the uncertainty in the placement of the continuum. The upper limits refer to 3σ values of the noise in the normalized spectrum. Figure 4 is a montage of different positions of the normalized spectrum resulting from the average of the three red exposures with the best S/N ratios. We have included the feature at $\lambda = 6206 \text{ \AA}$, although not a class A of Herbig, because it is blended with $\lambda 6203$. Most of the bands are clearly detected at the velocity of the gas in Cen A. The bands at $\lambda 6269$ and $\lambda 6283$ are heavily contaminated by O₂ atmospheric absorption. The DIBs which have the narrowest width according to Herbig (1975) are beginning to be resolved into

Table 2. Ca II and Na I absorption components in the spectrum of SN 1986G and NGC 5128

| Component number | Profile decomposition | | | Computed equivalent widths | | Measured equivalent widths | |
|------------------|---------------------------------|-------------------------------|---|---|---|---|---|
| | v_H (km s^{-1}) | b (km s^{-1}) | $N(\text{Ca}^+)$ (10^{11} cm^{-2}) | $W_\lambda(\text{K})$ ($\text{m}\text{\AA}$) | $W_\lambda(\text{H})$ ($\text{m}\text{\AA}$) | $W_\lambda(\text{K})$ ($\text{m}\text{\AA}$) | $W_\lambda(\text{H})$ ($\text{m}\text{\AA}$) |
| (1) | (2) | (3) | (4) | (5) | (6) | (7) | (8) |
| <i>Ca II</i> | | | | | | | |
| 1 | – 45: | 13: | 5.4: | 48 | 25 | 384 ± 2 ^a | 258 ± 3 |
| 2 | – 11.5 | 13 | 68.0 | 348 | 230 | | |
| 3 | + 97 | 5 | 1.9 | 17 | 9 | 17 ± 1.5 | 9 ± 2 |
| 4 | + 236 | 8 | 4.0 | 35 | 18 | 91 ± 2 | 34 ± 2.5 |
| 5 | + 257 | 15 | 5.5 | 49 | 25 | | |
| 6 | + 310 | 8 | 4.0 | 35 | 18 | 32.5 ± 1.5 ^b : | ... ^c |
| 7 | + 340: | 7: | 2.5: | 22 | 12 | 1079 ± 2 | 728 ± 4 |
| 8 | + 373 | 13 | 65.0 | 340 | 223 | | |
| 9 | + 414 | 11 | 43.0 | 251 | 158 | | |
| 10 | + 439: | 8: | 13.0: | 98 | 55 | | |
| 11 | + 455: | 4.5: | 8.0: | 59 | 34 | | |
| 12 | + 482 | 16 | 63.0 | 366 | 231 | | |
| Component number | Profile decomposition | | | Computed equivalent widths | | Measured equivalent widths | |
| (1) | v_H (km s^{-1}) | b (km s^{-1}) | $N(\text{Na}^+)$ (10^{11} cm^{-2}) | $W_\lambda(\text{D}_2)$ ($\text{m}\text{\AA}$) | $W(\text{D}_1)$ ($\text{m}\text{\AA}$) | $W_\lambda(\text{D}_2)$ ($\text{m}\text{\AA}$) | $W_\lambda(\text{D}_1)$ ($\text{m}\text{\AA}$) |
| <i>Na I</i> | | | | | | | |
| 1 | – 45 ^d | 13 ^d | ≲ 0.5 ^e | ≲ 10 | ≲ 5 | ≲ 10 ^e | ... |
| 2 | – 6.5 | 7 | ≲ 65 | 400 | 316 | 399 ± 2 | 317 ± 1 |
| 3 | + 97 ^d | 5 ^d | ≲ 0.3 ^e | ≲ 6 | ≲ 3 | ≲ 6 ^e | ... |
| 4 | + 236 ^d | 8 ^d | 1.3 | 26 | 13 | 63 ± 1 | 32: |
| 5 | + 257 ^d | 15 ^d | 2.4 | 47 | 24 | | |
| 6 | + 310 | 8 ^d | 1.2 | 24 | 12 | blended | 12 |
| 7 | + 340: ^d | 7: ^d | ≲ 0.6 ^e | ≲ 12 | ≲ 6 | ⊕ ^f | ≲ 6 ^e |
| 8 | + 375 | 10 | 120 | 609 | 496 | 2061 ± 2 | 1756 ± 2 |
| 9 | + 414 | 7 | 120 | 455 | 386 | | |
| 10 | + 439: | 5: | 5.0: | 84 | 45 | | |
| 11 | + 459 | 4.5 | 40 | 252 | 196 | | |
| 12 | + 488 | 10 | 260 | 706 | 618 | | |

^a Random 1σ errors to the equivalent widths, corresponding to the measured signal-to-noise ratios of the spectra. Systematic errors from the uncertainty in the continuum placement are generally 3–5 times larger

^b Feature partially blended

^c Affected by a cosmic ray event

^d Adopted from the Ca II fit

^e Upper limits deduced from consideration of the signal-to-noise ratio of the spectrum in the region of interest and of blending with nearby features (telluric and interstellar)

^f Blended with water vapour absorption feature

the strongest components detected in the Ca II and Na I absorptions at the velocity of Cen A, but a measurement of the relative intensity is not possible. A discussion of the strengths of these features is given by di Serego Alighieri and Ponz (1987). A detailed, comparative analysis of these observations with similar ones in the Galaxy and in the Magellanic Clouds will be given elsewhere.

3.3. Discovery of molecular absorption lines

As discussed above and suggested by the conspicuous dust lanes seen in the optical images, the light path to the SN 1986G is affected by a strong reddening taking place in the disc of NGC 5128. In the central region of the galaxy several species of molecules (OH, H₂CO, and C₃H₂) have been detected in absorp-

Table 3. $N(\text{Ca}^+)/N(\text{Na}^0)$ in the different absorption components

| Component number | v_H (km s ⁻¹) ^a | $N(\text{Ca}^+)/N(\text{Na}^0)$ |
|------------------|--|---------------------------------|
| 1 | - 45: | ≥ 11 : |
| 2 | - 9 | 1.05 |
| 3 | + 97 | ≥ 6 |
| 4 | +236 | 3.1 |
| 5 | +257 | 2.3 |
| 6 | +310 | 3.3 |
| 7 | +340 | ≥ 4 : |
| 8 | +374 | ≥ 0.6 |
| 9 | +414 | ≥ 0.4 |
| 10 | +439: | 2.6: |
| 11 | +457 | 0.20: |
| 12 | +485 | ≥ 0.3 |

^a Average of Ca II and Na I velocities for each component

Table 4. Diffuse interstellar bands in the spectrum of SN 1986G

| Wavelength (Å) | W_{Galaxy} (mÅ) | W_{CenA} (mÅ) |
|----------------|--------------------------|------------------------|
| 5705.1 | ≤ 15 | 79 ± 5 |
| 5780.4 | 74 ± 5 | 335 ± 5 |
| 5797.0 | 36 ± 5 | 151 ± 5 |
| 5849.8 | ≤ 15 | 36 ± 5 |
| 6010.9 | ≤ 20 | 76 ± 8 |
| 6195.9 | 20 ± 8 | 30 ± 15 |
| 6203.1+6206.5 | $\leq 40^a$ | 191 ± 5 : |
| 6376.1+6379.3 | ≤ 40 | 75 ± 8 |

^a Partially blended with the Cen A component of the band at 6195.9 Å

Table 5. Equivalent widths of molecular absorption lines at NGC 5128 velocities

| Lines | EW (mÅ) | $3\sigma^a$ (mÅ) |
|-----------------|---------|------------------|
| CH | | |
| 4300.32 Å | 25 | 7 |
| CH ⁺ | | |
| 3957.70 Å | 19 | 7 |
| 4232.54 Å | 36 | 6 |

^a Computed with the formula $3\sigma = \frac{3\Delta I}{100} \cdot \frac{\lambda}{c} \cdot \Delta v$, where $\Delta I/100$ is the average N/S ratio in the adjacent continuum and Δv is the instrumental FWHM in km s⁻¹

tion at radio wavelengths against the strong nuclear radio source (Gardner and Whiteoak, 1976; van der Hulst et al., 1983; Seaquist and Bell, 1986). CO and C₃H₂ have also been detected in emission (Phillips et al., 1987; Bell and Seaquist, 1988). It was therefore of interest to search our high S/N spectra for molecular lines. The lines of CN $\lambda\lambda 3874.61, 3874.00, 3875.76$, CH $\lambda\lambda 4300.32, 3890.21, 3878.77, 3886.41$ and CH⁺ $\lambda\lambda 4232.54, 3957.70$ were chosen from a

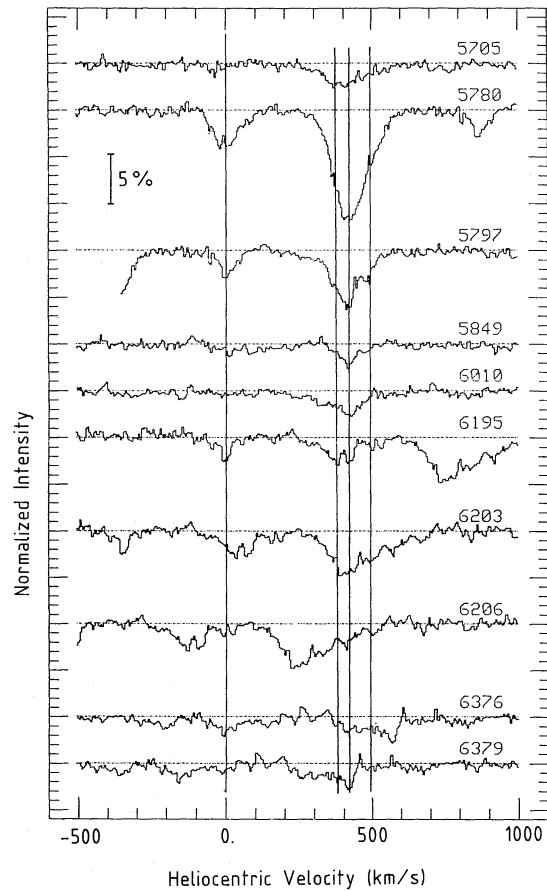


Fig. 4. The most prominent Diffuse Interstellar Bands in the range 5500–6500 Å in the spectrum of SN 1986G plotted on a common velocity scale. The dotted lines mark the estimated continuum level used for the normalization of the spectra. The vertical lines mark the expected positions of the bands at the average redshifts of the strongest components of Na I and Ca II

compilation of Cardelli and Wallerstein (1986) as possible candidates; of these CH $\lambda 4300.32$ and CH⁺ $\lambda\lambda 3957.70, 4232.54$ are identified at the velocities of the interstellar gas in NGC 5128 and their equivalent widths are given in Table 5.

Figure 5 shows the portions of the average blue spectrum of the supernova which include the detected molecular lines. To our knowledge this is the first detection of optical molecular lines in an extragalactic object beyond the Local Group. A subsequent detection of molecular lines in the LMC toward SN 1987A is discussed by Magain and Gillet (1987). There is an overall correlation between the stronger components seen in the Na I absorption and the structure observed in the molecular lines. A discussion of the relative intensity of the components is however not possible because of the large uncertainty in the equivalent widths of the individual components.

4. Location and origin of the various interstellar clouds

In this section we use the information provided by component velocities and column densities deduced in Sect. 3.1 above, to discuss the nature of the obvious interstellar clouds identified in the line of sight to the supernova. Because of the uncertainty in the determination of the column densities discussed above, the abundance ratios $N(\text{Ca}^+)/N(\text{Na}^0)$ can be in error as much as

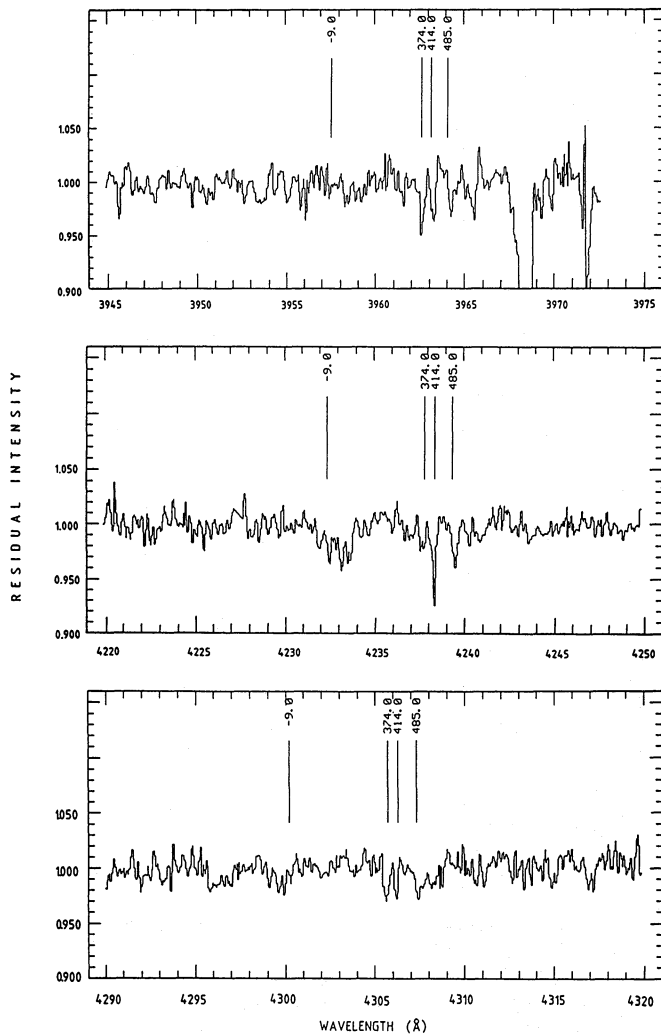


Fig. 5. Normalized portions of the average spectrum of SN 1986G encompassing the molecular lines CH⁺ $\lambda\lambda$ 3957.70, 4232.54 and CH λ 4300.32. The vertical lines mark the expected positions of the lines at the average radial velocity of the strongest components of Na I and Ca II. The strong absorption line at $\sim\lambda$ 3968.4 is the galactic component of the K Ca II line

50%. The conclusions we draw in the next sections are not significantly affected by the presence of errors of this magnitude.

4.1. Absorption by galactic gas

At galactic coordinates $l = 309.54$, $b = +19.40$, the sight-line to SN 1986G samples the interstellar medium of our Galaxy over an extended pathlength through the disk and halo. As can be seen from Fig. 6, the velocities of components 1, 2, and 3 are in excellent agreement with those expected for material distributed along the line of sight and sharing in the differential rotation of the Galaxy (we refer the reader to DPP for a description of the rotation model adopted and for a discussion of its limitations). In particular, the continuous absorption between $v_H = -9$ and -45 km s^{-1} evident in Ca II (see Fig. 3) apparently argues against a fast decrease in rotational velocity with increasing height above the plane. This is also the case for the gas towards M83 observed by DPP. While we cannot exclude the possibility that in this general direction there are interstellar clouds with large peculiar velocities, the present data do not provide evidence in support of

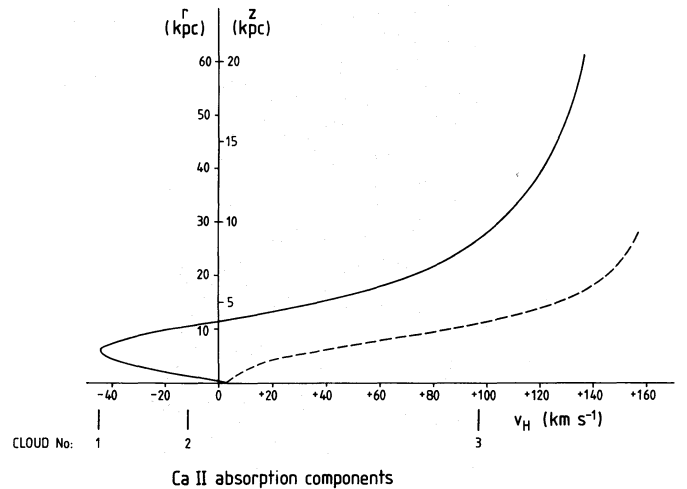


Fig. 6. Velocities expected for galactic interstellar gas in the direction of SN 1986G ($l = 309.54$, $b = +19.40$) as a function of the distance from the Sun, r , and projected distance above the galactic plane, z (both given on the ordinate). The two curves shown correspond to two extreme possibilities for the bulk motion of halo gas: corotation with the disk (continuous line), for which we adopted a flat rotation curve with $v = 220 \text{ km s}^{-1}$ at galactocentric distances $R > 4 \text{ kpc}$; and a fast exponential decrease in rotational velocity with distance from the plane, with scale height $h = 4 \text{ kpc}$ (broken line). The velocities of the first three components of the Ca II interstellar lines are indicated

the view that the halo rotates more slowly than the disk (e.g. de Boer and Savage, 1983; Savage and Massa, 1987).

It is interesting to note that, on the basis of its velocity, component number 3 ($v_H = +97 \text{ km s}^{-1}$) would appear to be located between ~ 4 and $\sim 9 \text{ kpc}$ above the plane (corresponding to ~ 12 and $\sim 28 \text{ kpc}$ from the Sun), depending on the kinematical model adopted. The weakness of Na I absorption in components 1 and 3 (see Table 3) cannot help discriminate between the alternative views that they originate in (a) nearby clouds with deviant motions from the large-scale rotation of the Galaxy; or (b) distant material partaking in the rotation and, therefore, appearing at a high velocity relative to the local standard of rest. In both cases, we would in fact expect an enhanced Ca⁺/Na⁰ ratio relative to low-velocity disk clouds, most likely reflecting a reduced proportion of Ca locked up in grains (Pettini et al., 1977; Shull et al., 1977; Hobbs, 1983; McGee et al., 1983; Van Steenberg and Shull, 1988).

4.2. Absorption by interstellar gas in NGC 5128

The complex set of absorption components at velocities between $v_H = 374$ and 485 km s^{-1} most likely arises in interstellar clouds in the disk component of Cen A.

Before relating the interstellar velocities to the known kinematics of the disk and dustband, it is important to note that multiple interstellar components, spanning $\geq 100 \text{ km s}^{-1}$ near the velocity of the parent galaxy, are not uncommon in the spectra of extragalactic supernovae. For example, towards SN 1983N in M83 (a late-type spiral viewed nearly face-on), DPP found seven components over $\sim 230 \text{ km s}^{-1}$, which they attributed to shocked interstellar gas possibly associated with a foreground H II region in that galaxy. The absorption we see towards SN 1986G in Cen A differs in one important aspect, however. As can be seen from Table 3, four out of the five components with $v_H \geq 374 \text{ km s}^{-1}$ exhibit very low $N(\text{Ca}^+)/N(\text{Na}^0)$ ratios, in the range 0.20 to 0.54 (whereas in the high-velocity gas in M83 this ratio has values

between ~ 3 and ≥ 6.5). Such low values are typical of dense and undisturbed interstellar clouds in the disk of the Milky Way (e.g. Hobbs, 1978). We see no evidence here of the disruption of dust grains commonly associated with interstellar shocks producing an enhanced gas-phase abundance of Ca (see also the discussion in Sect. 4.3 below). Consequently, we consider it more likely that the existence of these four low-ionisation components in SN 1986G is an indication of an extended pathlength through the gaseous disk of Cen A.

From Fig. 5 of Bland et al. (1987) it can be seen that the SN lies close to the kinematic line of nodes at a projected distance of $110''$ from the centre of NGC 5128 (taken to be at coordinates RA = $13^{\text{h}}22^{\text{m}}31^{\text{s}}.3$ and Dec = $-42^{\circ}45'35''$, epoch 1950.0; Bland, 1985). The velocity of H α emission at the SN position is $v_{\text{H}} \simeq 385 \text{ km s}^{-1}$, taking the average of the measurements by Marcellin et al. (1982); Bland et al. (1987) and di Serego Alighieri (1987, private communication). Consequently, material in front of the SN should appear at velocities progressively higher than $v_{\text{H}} = 385 \text{ km s}^{-1}$ with increasing radial distance up to a maximum defined by the systemic velocity of the galaxy, which we take to be $v_{\text{H}} = 545 \pm 10 \text{ km s}^{-1}$ from the redshift compilation by Hesser et al. (1984).

This is in qualitative agreement with the pattern of interstellar velocities we observe. In particular, it seems plausible to associate component 8, at $v_{\text{H}} = 374 \text{ km s}^{-1}$, with the interstellar gas in the inner regions producing the H α emission at $v_{\text{H}} = 385 \text{ km s}^{-1}$. The difference from the systemic velocity is well within the rotation curve of Cen A, which reaches a maximum rotational velocity of 260 km s^{-1} at a distance of $100''$ from the centre and remains constant up to $\sim 250''$ (Bland, 1985, and references therein).

Of course, if the interstellar medium in Cen A were confined to a thin flat disk, we would not expect such a wide range of velocities as observed. However, the complex velocity field of the emission line gas studied with TAURUS has been shown by Bland (1985) to be indicative of a warped disk geometry. The interstellar data presented here offer further support for Bland's model. The multiple components seen in the interstellar absorption lines can be most easily explained if the line of sight to the supernova intersects the warped disk at several locations.

Indeed, extrapolation of Bland's model of the ionized gas from radial distances of $\sim 250''$ (the limit of the TAURUS data) to $\sim 600''$, so as to reproduce the morphology of the dust lane (Nicholson and Taylor, 1987, private communication), predicts – in the direction of the supernova – a second component redshifted by $\sim 110 \text{ km s}^{-1}$ relative to that at $v_{\text{H}} = 374 \text{ km s}^{-1}$. This is in excellent agreement with the velocity of component 12 of the interstellar lines (at $v_{\text{H}} \simeq 485 \text{ km s}^{-1}$) which, furthermore, shows the highest column density of neutral sodium and the lowest value of the $N(\text{Ca}^+)/N(\text{Na}^0)$ ratio of all the components detected. This leads us to speculate that component 12 may arise in interstellar clouds associated with the dust lane in the warped disk of Cen A. Neither our data, however, nor the TAURUS model can be used to decide if this material is located in front or behind (or both!) the gas in the inner regions of the disk (moving at $v_{\text{H}} = 374 \text{ km s}^{-1}$), since in both cases a net redshift of $\simeq 110 \text{ km s}^{-1}$ would result. Furthermore, the warped disk model does not at present account for the third major component of the interstellar lines in Cen A at $v_{\text{H}} = 414 \text{ km s}^{-1}$ (component number 9).

Independent evidence that the SN is located behind much of the interstellar gas in this direction is also provided by the comparison of the reddening with the H I column density. Phillips et al. (1987) estimate $E(B-V) = 0.90 \pm 0.10 \text{ mag}$ from consideration of the SN colours; of this, 0.12 mag is due to our Galaxy

(Burstein and Heiles, 1984). If the Milky Way and NGC 5128 have similar overall gas-to-dust ratios ($N(\text{H I})/E(B-V) = 5.2 \cdot 10^{21} \text{ cm}^{-2} \text{ mag}^{-1}$) (Shull and Van Steenberg, 1985), we would anticipate a column density of neutral gas $N(\text{H I}) \simeq 5 \cdot 10^{21} \text{ cm}^{-2}$. This compares well with $N(\text{H I}) \simeq 10^{22} \text{ cm}^{-2}$ measured by van Gorkom (1987, private communication) from 21 cm data.

In this discussion we have not considered components 6 and 7 at $v_{\text{H}} = 310$ and 340 km s^{-1} . Clearly it is very difficult to come to a firm conclusion as to their location. Their velocities are sufficiently close to $v_{\text{H}} = 374 \text{ km s}^{-1}$ to make an origin in Cen A at least plausible. Interstellar clouds with motions which depart from galactic rotation by $35\text{--}65 \text{ km s}^{-1}$ are commonly seen in the local interstellar medium (e.g. Siluk and Silk, 1974). On the other hand, their $N(\text{Ca}^+)/N(\text{Na}^0)$ ratios are very similar to those of components 4 and 5 which are found at intermediate velocities between the Milky Way and NGC 5128. The hypothesis on the nature of these two latter components discussed in the following paragraph could indeed apply to components 6 and 7 as well.

4.3. Absorption at $v_{\text{H}} = 236$ and 257 km^{-1} : high velocity clouds in Centaurus A or intergalactic clouds?

From the discussion in Sects. 4.1 and 4.2 above it is apparent that the velocities of components 4 and 5 cannot be accommodated within the rotation curves of either the Milky Way or NGC 5128. From Fig. 6 it can be seen that the two components, if located in our Galaxy, have excess velocities of more than 73 and 94 km s^{-1} relative to differential rotation. Similarly, their velocities differ by 138 and 117 km s^{-1} respectively from that of component 8, which we have identified with the interstellar medium close to the line of nodes in the disk component of Cen A. In either case clouds 4 and 5 would be moving outwards from their parent galaxy, unless the supernova were located on the far side of Cen A, behind some infalling high-velocity gas. However, the latter seems a rather contrived scenario, especially in view of the absence of absorption at velocities higher than the systemic velocity of Cen A, as would be expected for infalling material on the near side of that galaxy (as viewed from the Sun).

Gas clouds moving with velocities as high as 150 km s^{-1} out of the disk of the large spiral galaxy M101 have been detected at 21 cm by van der Hulst and Sancisi (1988). Their origin is not yet understood and different hypotheses, such as a burst of SN explosions or dynamical instabilities from the interaction with a companion galaxy on the disk dynamics, have been considered. Our components 4 and 5 could represent the same type of objects given the similarity in the galaxy type and the suggestion put forward in the literature that the structure of Cen A be also the result of the interaction of two galaxies. On the other hand, their velocities, being intermediate between those of the Milky Way and NGC 5128, can be more easily understood if they arise in intergalactic clouds, not directly associated with either galaxy. The measured values of $N(\text{Ca}^+)/N(\text{Na}^0)$ ratio in the two components favour this interpretation, for the following reason. As mentioned in Sect. 4.1 above, the Ca^+/Na^0 ratio exhibits a well-known velocity dependence, first recognized by Routly and Spitzer (1952), in the sense that the ratio increases with increasing peculiar velocity of the cloud producing the absorption (Siluk and Silk, 1974). This effect is now generally recognized as resulting from the disruption of interstellar grains in which most of the calcium is normally locked up, with the subsequent return of Ca atoms to the gaseous phase. Although the details of the grain destruction process are still not fully understood (see McKee et al., 1987, for a recent treatment of this problem), if the velocities of

Table 6. Extragalactic sight-lines with Ca II absorption at $v_H > 200 \text{ km s}^{-1}$

| Galaxy | l | b | v_H | v_{LSR} | v_{GSR}^a | $\frac{N(\text{Ca}^+)}{N(\text{Ca}^0)}$ | Ref. |
|------------------|--------|--------|------------------------|------------------------|------------------------|---|------|
| (1) | (deg) | (deg) | (km s^{-1}) | (km s^{-1}) | (km s^{-1}) | (7) | (8) |
| NGC 3783 | 287.46 | +22.95 | +249 | +241 | + 48 | 1.7 | a, b |
| Fairall 9 | 295.10 | -57.83 | +201 | +190 | + 84 | ≥ 6 | c, d |
| NGC 5128 (Cen A) | 309.54 | +19.40 | +236 | +233 | + 73 | 3.1 | e |
| | | | +257 | +254 | + 94 | 2.3 | e |
| NGC 5236 (M83) | 314.58 | +31.97 | +248 | +249 | +116 | ≥ 2 | f |

^a Galactocentric velocity: $v_{\text{GSR}} = v_{\text{LSR}} + 220 \sin l \cos b$

References: (a) West et al. (1985), (b) Pettini, D'Odorico, and Brinks (in preparation), (c) Songaila (1981), (d) Morton and Blades (1986), (e) Present work, (f) DPP

components 4 and 5 were due to acceleration in interstellar shocks, either in the Milky Way or Cen A, we would expect $N(\text{Ca}^+)/N(\text{Na}^0)$ ratios in excess of ~ 10 (Hobbs, 1983), as measured for example in clouds in the vicinity of the Vela supernova remnant (Hobbs, Wallerstein and Hu, 1982). The fact that, on the contrary, components 4 and 5 exhibit only a mild Routly-Spitzer effect, in particular with values of $N(\text{Ca}^+)/N(\text{Na}^0)$ lower than those measured for components 1 and 3 (see Table 3), suggests that the velocities of the two components are more likely an indication of their extragalactic nature.

Similar arguments were put forward by West et al. (1985) and by DPP to argue for an extragalactic origin of the high velocity clouds they detected in front of NGC 3783 and SN 1983N in M83 respectively. Data of relevance to this question are collected in Table 6, which also includes absorption by the Magellanic Stream in front of Fairall 9.

DPP drew attention to the apparent coincidence in the values of heliocentric velocity v_H for the two clouds in line to NGC 3783 and M83 which have galactocentric velocities differing by 68 km s^{-1} (see Table 6). This could be interpreted as an indication that the absorption of $v_H = +248 \text{ km s}^{-1}$ is not extragalactic but occurs instead very close to the Sun, although there is no known mechanism for accelerating an interstellar cloud from rest to 250 km s^{-1} without disrupting its grain content. The present observations of Cen A, while providing data for a third sight-line, do not resolve this problem, since the values of v_{GSR} for components 4 and 5 are intermediate between those for NGC 3783 and M83, while the values of v_H are similar, but not actually the same, as those for the other two sight-lines.

If the clouds are intergalactic, the detection of Ca^+ and Na^0 is of considerable interest. Although uncertainties in the ionization balance of the gas, required to estimate the column densities of Ca^{2+} and Na^+ , and lack of measurements of corresponding H I prevent estimates of their metallicities, the clouds have obviously undergone at least some metal enrichment. Furthermore, an association with the Magellanic Stream, considered as a possibility by West et al. (1985) for the cloud in line to NGC 3783, becomes progressively less likely as more examples are found in directions, such as M83 and Cen A, which are further from the plane of the Stream.

In recent years 21 cm emission observations have led to the discovery of some convincing examples of intergalactic H I clouds (e.g. Mirabel and Cohen, 1979; Hart et al., 1980; Schneider et al.,

1983). Clearly it would be of great interest to search for associated metal lines. Chemical enrichment of the intergalactic medium by the winds of low-mass galaxies, whose gravitational fields may be insufficient to retain the products of supernova explosions and stellar mass loss, has been proposed by a number of authors and could have important consequences for galactic evolution (e.g. Silk et al., 1987).

5. Concluding remarks and suggestions for future work

The detailed observations of the rich interstellar absorption in the optical region in the direction of the SN 1986 G have provided new insights on the distribution and composition of gas in a late spiral galaxy and in the intergalactic and galactic medium.

The discovery of clouds at $v_{\text{He}} \simeq 240 \text{ km s}^{-1}$ has provided additional evidence for the existence of a complex structure of high velocity gas clouds centered at about $b = 20^\circ$ and possibly extending from galactic longitude $l = 280$ to $l = 315$. We cannot but stress the importance of the related 21 cm observations in this area of the sky and in particular in the direction of M83 and NGC 5128 to derive the column densities and the velocities of the neutral hydrogen. These data will help to discriminate between the three hypotheses we have considered: extragalactic clouds associated with the Local Supercluster or the remnant of a relatively local, energetic event in the disc of our galaxy or of NGC 5128.

Regarding the gas associated to NGC 5128, our data confirm the notion that a line of sight through the disc of a late type galaxy is likely to intercept several clouds of gas at velocities spanning $\geq 100 \text{ km s}^{-1}$ near the velocity of the parent galaxy, and these clouds can be detected in the intrinsically weak lines such as the Ca II and Na I doublets, if the S/N ratio and the resolution are sufficiently high. This point is illustrated in Table 7 where we have summarized the information on the structure of the interstellar medium in late type galaxies as derived from observations of a background source at a resolving power larger than 10000 and sufficiently good S/N ratio. In all cases the background sources were supernovae brighter than 15 mag, a fact that shows the unique opportunity offered by these transient events. As the supernovae locations might have been not fully behind the parent galaxy the numbers of detected components and the velocity spans in Table 7 actually represent lower limits. Most of the clouds are detected both in Ca^+ and Na^0 absorption but as the cases of M83 and NGC 5128 have clearly shown, the relative strength of the column densities of the two elements can vary over a wide range

Table 7. Interstellar gas in late-type galaxies as seen in the spectra of associated supernovae

| SN | Galaxy | R^a (kpc) | Resolving power ^b | # Components | | Velocity span ^c (km s ⁻¹) | References |
|-------|----------|----------------|---------------------------------|--------------|------|--|------------|
| | | | | Ca II | Na I | | |
| 1983N | M83 | 3.1 | 20000 (70) | 7 | 4 | 230 | DPP |
| 1984J | NGC 1559 | 3 | 16000 (30) | 5 | 5 | 200 | 1 |
| 1986G | NGC 5128 | 2: | 20000 (100) | 7 | 7 | 170 | This paper |
| 1987A | LMC | | 100000 (300) | 10 | 7 | 90 | 2 |

^a Projected distance from the centre of the parent galaxy

^b Average S/N ratio of the observations in parenthesis

^c As indicated from the Ca II components

References: 1) D'Odorico and Bergeron (in preparation); 2) Vidal-Madjar et al. (1987)

from one component to the other depending on the location of the clouds.

QSOs represent in principle another class of ideal background sources for the study of the interstellar matter in galaxies. Very few quasars, however, have been identified close to galaxies and their magnitudes are such that it is not possible in most cases and with present 4 m class telescopes to obtain data comparable with those we have discussed here. The study of the galaxy-QSO pair 1327-206 by Bergeron et al. (1987) is a recent example of such an investigation and of its limitations. The observations of the interstellar absorption in gas rich galaxies like the ones presented here are also useful to interpret the metal absorption systems seen at high redshifts in the spectra of QSOs.

Finally, this work presents the first measurements of interstellar DIBs and molecular lines at optical wavelengths in the interstellar medium outside the Local Group galaxies. In the case of the DIBs it appears of particular interest to search for these features in the spectra of future bright supernovae, as the correlation of their strengths with other properties of the parent galaxies, such as the Ca and Na interstellar absorption, the H I and molecular content and the amount of reddening, is likely to give useful clues to their origin.

Acknowledgements. We wish to thank D. Malin for the photograph of SN 1986G reproduced in Fig. 1 and G. Wallerstein for useful discussions.

References

- Bell, M. B., Seaquist, E. R.: 1988 (preprint)
- Bergeron, J., D'Odorico, S., Kunth, D.: 1987, *Astron. Astrophys.* **180**, 1
- Bertola, F., Galletta, G., Zeilinger, W. W.: 1985, *Astrophys. J.* **292**, L51
- Blanco, V. M.: 1986, *IAU Circular* 4224
- Bland, J.: 1985, PhD. Thesis, University of Sussex, England
- Bland, J., Taylor, K., Atherton, D. O.: 1987, *Monthly Notices Roy. Astron. Soc.* **228**, 595
- Bues, I., Duerbeck, H. W., Kohoutek, L.: 1986, *IAU Circular* 4214
- Burstein, D., Merles, C.: 1978, *Astrophys. J.* **225**, 40
- Cardelli, J. A., Wallerstein, G.: 1986, *Astrophys. J.* **302**, 492
- Craggs, T.: 1986, *IAU Circular* 4208
- de Boer, K. S., Savage, B. D.: 1983, *Astrophys. J.* **265**, 210
- de Vaucouleurs, G.: 1979, *Astrophys. J.* **74**, 1270
- de Vaucouleurs, G., Corwin, H. G., Jr.: 1975, *Astrophys. J.* **202**, 327
- di Serego Alighieri, S., Ponz, D.: 1987, *Proc. ESO Workshop on SN 1987A*, ed. J. Danziger, p. 545
- D'Odorico, S., Tannè, J. F.: 1984, ESO Operating Manual No. 2
- D'Odorico, S., Ponz, D.: 1984, *ESO Messenger* **37**, 29
- D'Odorico, S., Pettini, M., Ponz, D.: 1985, *Astrophys. J.* **299**, 852
- Ebnetter, K., Balick, B.: 1983, *Publ. Astron. Soc. Pacific* **95**, 675
- Evans, R.: 1986, *IAU Circular* 4208
- Feast, M. W., Phillips, M.: 1986, *IAU Circular* 4210
- Gardner, F. F., Whiteoak, J. B.: 1976, *Monthly Notices Roy. Astron. Soc.* **175**, 9P
- Hart, L., Davis, R. D., Johnson, S. C.: 1980, *Monthly Notices Roy. Astron. Soc.* **191**, 269
- Herbig, G. H.: 1975, *Astrophys. J.* **196**, 129
- Hesser, J. E., Harris, H. C., van den Bergh, S., Harris, G. L. H.: 1984, *Astrophys. J.* **276**, 491
- Hobbs, L. M.: 1978, *Astrophys. J. Suppl.* **38**, 129
- Hobbs, L. M., Wallerstein, G., Hu, E. M.: 1982, *Astrophys. J. Letters* **252**, L17
- Hobbs, L. M.: 1983, *Astrophys. J.* **265**, 317
- Jenkins, E. B., Rodgers, A. W., Harding, P., Morton, D. C., York, D. C.: 1984, *Astrophys. J.* **281**, 585
- Magain, P., Gillet, D.: 1987, *Astron. Astrophys.* **184**, L5
- Marcelin, M., Boulesteix, J., Courtes, G., Milliard, B.: 1982, *Nature* **297**, 38
- Mathewson, D. S., Cleary, M. N., Murray, J. D.: 1974, *Astrophys. J.* **190**, 291
- McGee, R. X., Newton, L. M., Morton, J. C.: 1983, *Monthly Notices Roy. Astron. Soc.* **205**, 1191
- McKee, C. F., Hollenbach, D. J., Seab, C. G., Tielens, A. G. G. M.: 1987, *Astrophys. J.* **318**, 674
- Merrill, P. W.: 1934, *Publ. Astron. Soc. Pacific* **46**, 206
- Mirabel, I. F., Cohen, R. J.: 1979, *Monthly Notices Roy. Astron. Soc.* **188**, 219
- Morton, D. C., Blades, J. C.: 1986, *Monthly Notices Roy. Astron. Soc.* **220**, 927
- Nachman, P., Hobbs, L. M.: 1973, *Astrophys. J.* **182**, 481
- Pettini, M., Boksenberg, A., Bates, B., McCaughan, R. F., McKeith, C. D.: 1977, *Astron. Astrophys.* **61**, 839
- Pettini, M., D'Odorico, S.: 1986, *Astrophys. J.* **310**, 700
- Phillips, M. M., Phillips, A. C., Heathcote, S. R., Blanco, V. M., Geisler, D., Hamilton, D., Suntzeff, N. B., Jablonski, F. J., Steiner, J. E., Cowley, A. P., Schmidtke, P., Wyckoff, S., Butchings, J. B., Tonry, J., Strauss, M. A., Thorstensen, J. R.,

- Boney, W., Maza, J., Ruiz, M.T., Rich, R.M., Grindlay, J.E., Cohn, H., Smith, H.A., Lutz, J.H., Saha, A.: 1987, *Publ. Astron. Soc. Pacific* **99**, 592
- Phillips, T.J., Ellison, B.N., Keene, J.B., Leighton, R.B., Howard, R.J., Masson, C.R., Sanders, D.B., Veidt, B., Young, K.: 1987, *Astrophys. J.* **322**, L73
- Ponz, D., Brinks, E., D'Odorico, S.: 1986, *Proc. SPIE Conf. No. 627*, p. 707
- Rich, R.M.: 1987, *Astron. J.* **94**, 651
- Routly, P.M., Spitzer, L.: 1952, *Astrophys. J.* **115**, 227
- Sandage, A.R., Tammann, G.A.: 1974, *Astrophys. J.* **194**, 551
- Savage, B.D., Massa, D.: 1987, *Astrophys. J.* **314**, 380
- Schneider, S.E., Helou, G., Salpeter, E.E., Terzian, Y.: 1983, *Astrophys. J. Letters* **273**, L1
- Seaquist, E.R., Bell, M.B.: 1986, *Astrophys. J.* **303**, L67
- Shull, J.M., York, D.G., Hobbs, L.M.: 1977, *Astrophys. J. Letters* **211**, L139
- Shull, J.M., van Steenberg, M.E.: 1985, *Astrophys. J.* **294**, 599
- Silk, J., Wyse, R.F.G., Shields, G.A.: 1987, *Astrophys. J. Letters* **322**, L59
- Siluk, R.S., Silk, J.: 1974, *Astrophys. J.* **192**, 51
- Songaila, A.: 1981, *Astrophys. J. Letters* **243**, L19
- van der Hulst, J.M., Golisch, W.F., Haschick, A.D.: 1983, *Astrophys. J. Letters* **264**, L37
- van der Hulst, T., Sancisi, R.: 1988, *Astron. J.* **95**, 1354
- Van Steenberg, M.E., Shull, J.M.: 1989, *Astrophys. J. Suppl.* (in press)
- Vidal-Madjar, A., Andreani, P., Cristiani, S., Ferlet, R., Lanz, T., Vladilo, G.: 1987, *Astron. Astrophys.* **177**, L17
- Vladilo, G., Crivellari, L., Molaro, P., Beckman, J.E.: 1987, *Astron. Astrophys.* **182**, L59
- West, K.A., Pettini, M., Penston, M.V., Blades, J.C., Morton, D.C.: 1985, *Monthly Notices Roy. Astron. Soc.* **215**, 481
- Wilkinson, A., Sharples, R.M., Fosbury, R.A.E., Wallace, P.T.: 1986, *Monthly Notices Roy. Astron. Soc.* **218**, 297